20 (2026) 100670

Contents lists available at ScienceDirect

Carbon Capture Science & Technology

journal homepage: www.elsevier.com/locate/ccst

Full Length Article

CO separation from complex streams enabled by dual-functional materials

Donato Pinto, José Palomo, Atsushi Urakawa *

Catalysis Engineering, Department of Chemical Engineering, Delft University of Technology, Van der Maasweg 9, 2629, HZ, Delft, the Netherlands

ARTICLE INFO

Keywords:
Carbon monoxide
Carbon monoxide separation
CO/N_2 separation
Carbon capture and utilisation
in situ DRIFTS
Dual-functional materials

ABSTRACT

We report a CO separation technology enabled by a dual-functional material (Cu-K/γ-Al_2O_3) under isothermal and isobaric conditions. The CO adsorption-desorption cycles were demonstrated in a fixed-bed reactor between 300 - 450 °C with the achievement of a full CO capture scenario (complete CO uptake until breakthrough). Sorbent regeneration with H_2 directly upgraded the captured CO into syngas (H_2 + CO). Mechanistic insights obtained from *in situ* diffuse reflectance infrared Fourier transform spectroscopy (DRIFTS) revealed that CO capture proceeds via interaction with surface hydroxyl intermediates, forming potassium carbonate species. Regeneration occurs through H_2 activation on the Cu sites and subsequent carbonate decomposition. The capability of handling humid and O_2-containing streams during CO capture was verified. As an alternative to H_2, water vapor can trigger sorbent regeneration after CO capture with release of gaseous CO_2, highlighting the additional system potentiality of full CO capture and conversion through a sorption mediated water-gas shift (WGS)-like process.

1. Introduction

The steady increase in post-combustion emissions released into the atmosphere has led to significant pollution and climate disruption (Filonchyk et al., 2024). CO_2, being the most abundant pollutant on a daily mass basis, has received a great deal of attention, with numerous initiatives and global political and social efforts directed towards mitigating its emissions to the atmosphere (Seneviratne et al., 2016). In this scenario, CO_2 capture technologies have emerged as reliable strategies for key sectors, such as the cement and steel industries, aiming to minimize the carbon footprint of the processes and improve sustainability. In particular, integrated carbon capture and utilization (ICCU) combines CO_2 capture with its further transformation, commonly using H_2, to produce key chemical building blocks such as CO, enabling the valorisation of CO_2 emissions (Bobadilla et al., 2016; Li et al., 2024; Sun et al., 2024).

In addition to carbon dioxide, carbon monoxide is frequently encountered as by-product in exhaust streams from industrial operation, refineries, processing of hydrocarbons, internal combustion engines and biomass gasification processes. In particular, CO is found in high concentration in waste streams from steel and iron production plants (*i.e.* blast furnace gas), accounting for up to 20–28% of the flue gas (Carpenter, 2012). Due to its toxicity and the difficulties associated with its separation using conventional technologies, CO is preferentially burned to CO_2 for heat recovery (Nogami et al., 2006; Schneising et al., 2024). However, this results in additional net CO_2 emissions that have to be handled by its subsequent sequestration and/or conversion technologies, such as the aforementioned ICCU process, which regenerates CO in the processed —captured and converted— stream, making it suitable for further chemicals production.

In this context, there is significant momentum behind capturing and directly reutilizing CO from waste streams, driven by the goal of further minimizing total carbon emissions and achieving a circular economy with a closed carbon loop (Kempken et al., 2021). For this aim, the sequestration of CO from such streams must be feasible. Traditional methods for gas separation include cryogenic distillation, separation membranes, absorption in liquid phase sorbents and adsorption on solid sorbents (Delgado and Arean, 2011; Evans et al., 2018; Li et al., 2023; Ramírez-Santos et al., 2018).

Cryogenic distillation and membranes have been applied for CO separation purposes. However, due to the similar molecular size and physical properties of N_2 and CO, those technologies fail in effectively separating those two molecules, especially in presence of high N_2 concentration in the gas source (James et al., 2023).

Absorption methods exploit the complexation of CO on Cu(I) ions in solution (Saeednia et al., 2025). The complexation —CO capture— takes place at ambient temperature and high pressure, while heating and reducing pressure promotes the release of the CO back to the gas phase.

* Corresponding author.
E-mail address: A.Urakawa@tudelft.nl (A. Urakawa).

https://doi.org/10.1016/j.ccst.2026.100670
Received 8 June 2026; Received in revised form 18 July 2026; Accepted 28 July 2026
Available online 28 July 2026

This methodology suffers from intrinsic limitations due to the instability of the Cu(I) ions and their susceptibility to poisoning molecules such as CO_2, O_2 and H_2O (Hirai et al., 2006; Ma et al., 2023). An example of this technology is the commercialized COSORB process that makes use of a cuprous aluminium chloride ($CuAlCl_4$) in toluene solution to selectively capture CO. Within this process, the removal of H_2O from the feed is critical to prevent the irreversible degradation of the salt, with formation of corrosive HCl (Ma et al., 2023).

Adsorption methods exploit the polarizability of the CO molecule to selectively adsorb it on a solid sorbent. The typical mechanism of adsorption involves the well-established formation of π-complexes between the CO molecule and transition metals (Chen et al., 2026; Scheijen et al., 2009; Smith and Quets, 1965), especially Cu(I). This strong, reversible interaction is exploited for different families of adsorbents, including Cu(I)-ion-exchanged zeolites, activated carbons and metal organic frameworks (Islamoglu et al., 2020; Ko et al., 2022; Peng et al., 2015). While CO can be effectively adsorbed at ambient temperature and pressure, achieving high capture capacities up to few mmol per gram (Bloch et al., 2014; Peng et al., 2015), the sorbent regeneration step typically imposes vacuum conditions (James et al., 2023). The need of switching temperature and pressure conditions to regenerate the sorbent material is a common feature of this CO separation technology, increasing both process complexity and the operational costs.

In the light of the current state of technology readiness, CO separation demands very specific operation conditions, including low temperatures for CO sorption, temperature and pressure swing for desorption, and the strict exclusion of certain chemical species for the proper and stable operation. These requirements are far from actual CO-containing waste streams, particularly those generated in post-combustion processes, which are usually generated at high temperatures, with carbon monoxide present in complex mixtures of gases that include N_2, H_2, O_2, CH_4, CO_2 and significant amounts of H_2O vapor (Kim et al., 2018). Consequently, there is lack of an effective technology to separate CO from waste streams containing complex mixtures (including N_2, CO_2, H_2O and O_2) and reutilizing it as a chemical source for CO demanding processes, such as Fischer Tropsch and methanol synthesis process (Nielsen et al., 2018).

In this work we present the performance of a novel chemisorption-based CO capture process to separate CO from complex mixtures (including N_2, O_2, H_2O) using a dual-functional material, operating at industrially relevant conditions, *i.e.* high temperature operation. *In situ* DRIFTS analysis provided evidence for the CO capture and sorbent regeneration mechanism. This process enables sorbent regeneration at the same temperature and pressure as separation (isothermal and isobaric operation), simplifying and potentially lowering the operational costs. The use of H_2 for the regeneration step allows the direct formation of syngas ($H_2 + CO$) at the reactor outlet. Therefore, this novel CO capture technology enables the reintegration of CO into the carbon cycle, contributing to carbon footprint reduction while ensuring compliance with environmental and regulatory standards for chemical processes.

2. Material and methods

2.1. Sorbent synthesis and characterization

Commercial aluminum oxide (γ-phase, Thermo Fisher) was used as support material. Cu and K were added in two steps through sequential incipient wetness impregnation. In the first step, support powder was impregnated with a copper nitrate trihydrate (Merck, > 99.5%) solution in milli-Q water, dried at 120 °C for 1 h and calcined at 500 °C for 5 h. The resulting Cu/Al_2O_3 powder was further impregnated with a potassium carbonate (anhydrous, Sigma, > 99.0%) solution in milli-Q water, dried at 120 °C for 1 h and calcined at 500 °C for 5 h.

Powder X-ray diffractograms were acquired on a Bruker D8 Advance diffractometer (Bragg-Brentano geometry) using monochromatic Cu Kα radiation (λ=1.5406 Å) in the range 5°−90° with a scan step of 0.05° Scanning Electron Microscopy – Energy Dispersive Spectroscopy measurements of the fresh samples were performed on a JEOL JMS-IT700 Field Emission Microscope operated in high vacuum mode with acceleration voltage set at 15.0 kV. Thermogravimetric analysis (TGA) was carried out in a METTLER TOLEDO SF/1100. The samples were heated at a rate of 10 °C min^{-1} up to 800 °C under 100 mL min^{-1} flow of N_2 or H_2 (5 vol% in Ar).

2.2. CO separation performance test

The sorption-regeneration tests were performed in a dedicated setup described in an earlier contribution (Pinto et al., 2024). A quartz tube reactor (ID 4 mm, OD 6 mm) was filled with 200 mg of catalyst material (pelletised, crushed and sieved to the size range of 200–300 μm) between quartz wool layers and placed into a reactor furnace. Gas inlet feed was controlled by a system of mass-flow controllers (Bronkhorst) and 4-way switching valves (VICI Valco). Fourier Transform InfraRed spectroscopy (Bruker ALPHA) and mass spectrometry (Omnistar Pfeiffer Vacuum) were used to analyse the reactor effluent.

Before each experiment, the sorbent material was pre-treated with pure H_2 (50 mL min^{-1}) for 30 min at 450 °C. Each cycle of operation consisted of alternation of diluted CO and pure H_2 feed, with He purging phases interposed between the reactant cycles. A total flowrate of 50 mL min^{-1} was maintained during the experiments. For the experiments including H_2O, a syringe pump was used to dose liquid water into the gas feed line at the reactor inlet through a rubber septum. The concentration profiles shown are averaged over multiple cycles after stable conditions of operations were achieved.

2.3. In situ DRIFT spectroscopy

In situ DRIFT spectroscopy experiments were performed on a ThermoScientific Nexus FTIR spectrometer employing liquid N_2-cooled MCT detector. 5 mg of sample were loaded into a Harrick DR high temperature cell equipped with CaF_2 windows. A total flowrate of 10 mL min^{-1} was maintained during the experiments. Prior to any experiment, the sample was pretreated in H_2 (30 vol% in Ar, total flowrate 30 mL min^{-1}) for 15 min. A background spectrum was acquired in pure H_2 at the end of the pretreatment and subtracted from the spectra acquired during the following reaction. A total flowrate of 10 mL min^{-1} was maintained during the experiments, alternating a diluted CO pulse (5 vol% in Ar) and a H_2 pulse (30 vol% in Ar).

3. Results and discussion

3.1. CO separation performance

A γ-Al_2O_3 supported Cu-K sorbent (Cu-K/Al_2O_3) was synthesized via incipient wetness impregnation, targeting a composition of 11 wt% Cu and 10 wt% K in the calcined material. Powder X-ray diffraction (See Supplementary Material Fig. S1) and SEM-EDS analysis (Fig. S2) indicate the presence of a well-dispersed or amorphous potassium phase while the excess loading of copper results in crystalline CuO agglomerates. The results are in agreement with previous studies on the system used for ICCU (Hyakutake et al., 2016; Pinto et al., 2024), which revealed drastic structural changes intervening upon exposure of the systems to H_2 at high temperatures, including redispersion of the metallic copper phase.

The CO separation performance of Cu-K/Al_2O_3 was investigated in a fixed-bed reactor configuration at different temperatures. Following activation under pure H_2 at 450 °C for 30 min, cyclic operation was carried out by alternately feeding a CO stream (2 vol% in He) and pure H_2, aiming to simulate sorption and regeneration, respectively. Inert He flushing phase was interposed between the active phases to investigate eventual spontaneous release of the adsorbed CO, and to ensure the non-

coexistence of the components from the two active streams. The whole process was executed under isothermal and isobaric (1 bar) conditions.

Fig. 1 presents the concentration of CO at the reactor outlet, measured by FTIR, as a function of time for the sorption-desorption cycles, at 350, 400 and 450 °C. The CO concentration profile of the blank experiment (empty grey squares in Fig. 1) is included as a reference for quantitative comparison. For all the analyzed temperatures, CO was fully captured by the sorbent, with no CO detected at the reactor outlet until saturation of the sorbent sites, after which a typical breakthrough profile for the adsorbate was observed. The breakthrough point shifted to longer times with increasing temperature, indicating a higher CO capture capacity at higher temperatures (Fig. 1, 450 °C). During the inert He pulse, no release of CO was observed at the reactor outlet. This highlights the strong, chemical nature of the interaction between the CO and the active sites of the sorbent. Conversely, the exposure of the saturated sorbent to H_2 triggered CO desorption, with no further component being released from the sorbent. As a result, direct generation of syngas (H_2 + CO) was achieved. The instantaneous composition of the generated syngas can be adjusted increasing the amount of sorbent – and thus increasing the captured CO per cycle – or by changing the volumetric H_2 flow, pointing out the potential of this approach for customizing H_2 to CO ratio in the generated stream. When comparing the CO concentration profile during the regeneration stage at different temperatures, it was found that this stage was strongly temperature dependent, with higher temperatures accelerating CO release kinetics and producing higher CO concentration peaks in the effluent. The CO capture capacity was calculated from the amount of CO released during the regeneration step in H_2. At 350 °C, the material exhibited a capture capacity of 0.12 mmol/g. When compared with traditional zeolites (13X: 0.5 mmol/g; 5A: 1.2 mmol/g) and MOFs alternatives (MOF-5: 0.15 mmol/g; MIL-100(Fe): 0.38 mmol/g; 0.8Cu(I)@MIL-100(Fe): 2.78 mmol/g) (Peng et al., 2015), this performance stands in the lower range of adsorption capacity. However, this reduced performance is highly compensated, in terms of process conditions, by the unique ability of capturing CO at high temperature and the non-vacuum regeneration conditions. A modest increase in CO adsorption capacity (mol of CO released in H_2 / g of sorbent) was detected, raising from 120 μmol/g (350 °C) to 150 μmol/g (450 °C). This trend may be associated with the higher degree of reduction of the sorbent active phases, leading to more capture sites. Thermogravimetric analysis (TGA) experiments were performed to explore the thermal stability of the sorbent materials under N_2 and H_2 flows. Fig. S3a reports the first derivative of the TGA profiles, representing the instantaneous rate of weight loss in function of the temperature. Compared to the N_2-TGA, exposing the Cu-K/Al_2O_3 sorbent to H_2 stimulated both the reduction of CuO and the decomposition of the K_2CO_3 phase at temperature higher than 250 °C. In line with previous results on the same system (Pinto et al., 2024), a synergy between the Cu and K phase was observed with two main effects. On one side, the higher reduction temperature of the CuO phase compared to unpromoted Cu/Al_2O_3 system (Fig. S3b); on the other side, the enhanced decomposition of the K_2CO_3 phase in presence of Cu. The latter process is the key for the generation of the active phase for CO capture.

3.2. *Mechanistic insights on CO capture via in situ DRIFT spectroscopy*

As demonstrated above, Cu-K/Al_2O_3 enables effective CO capture from a CO-containing streams, achieving complete uptake, with no CO in the effluent, until sorbent saturation (breakthrough point). Cu-K/Al_2O_3 sorbents have been investigated for the purpose of CO_2 capture and reduction processes (Hyakutake et al., 2016), with the K phase identified as the active component for CO_2 capture (Pinto et al., 2024). In these systems, the dispersion of K_2CO_3 on the Al_2O_3 support induces a destabilisation of the carbonate compared to its bulk state, causing supported K_2CO_3 to be reduced in H_2 at substantially lower temperatures than bulk K_2CO_3 (Pinto et al., 2024; Veselovskaya et al., 2013). On the other hand, the transition metal in the Cu-K/Al_2O_3 has been claimed to act as a H_2 activator, accelerating the decomposition of the K_2CO_3 species, hence making the process feasible for sorption-regeneration cycles.

In situ DRIFTS experiments were conducted in the present study to identify the dynamic of surface intermediates on the Cu-K/Al_2O_3 sorbent during the cycling of CO and H_2 streams (*i.e.* CO capture and sorbent regeneration steps) at high temperature. Fig. 2 reports the DRIFT spectra acquired during a cycle of operation at 450 °C. An initial baseline spectrum, acquired at the end of the pretreatment in H_2, was subtracted to the measurement in order to display the relative changes in surface intermediates associated with the capture and regeneration steps. During the CO pulse (Fig. 2a, 0–10 min), the capture of CO was accompanied with a strong increase in the intensity of bands appearing in the carbonate region (1800–1000 cm^{-1}). Among the most prominent features, two main broad bands centred at around 1590 and 1325 cm^{-1} and a lower intensity band around 1050 cm^{-1} were observed. These bands are characteristic features of bidentate carbonate species, as identified in similar systems (Busca and Lorenzelli, 1982; Fedorova et al., 2024; Montanari et al., 2011). The splitting value of the doubly degenerated asymmetric CO stretching vibration of carbonates (bands centered at 1590 and 1325 cm^{-1}) confirms this assignment (Coenen et al., 2018). Switching the atmosphere to H_2 (Fig. 2a, 10–20 min) triggered CO

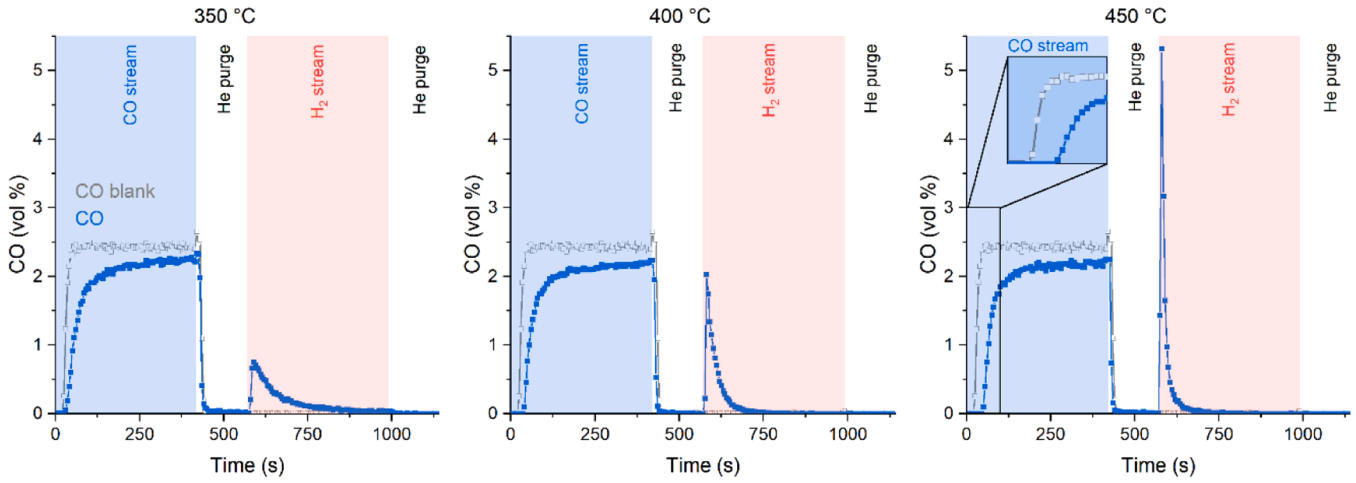

Fig. 1. CO separation performance with temperature. FTIR analysis of reactor effluent during sorption-regeneration tests over Cu-K/Al_2O_3 at 350 °C (left), 400 °C (middle) and 450 °C (right), showing CO concentration during separation tests (blue squares) and blank test at room temperature (empty grey squares). Tests consisted of cyclic alternation of CO stream, He purge and pure H_2 stream.

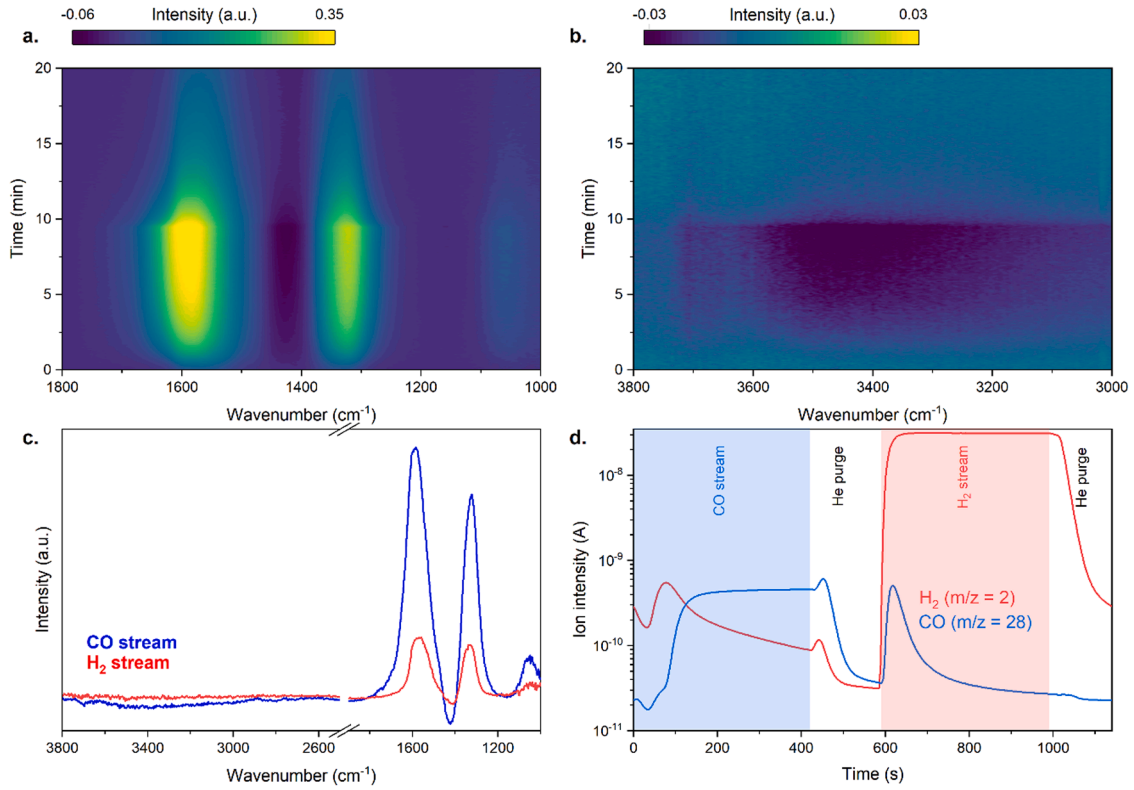

Fig. 2. *In situ* DRIFTS experiment. Drifts experiment over Cu-K/Al_2O_3 during CO (5 vol% in He, 0–10 min)- H_2 (30 vol% in Ar, 10–20 min) pulses at 450 °C. a. Carbonate region (1800–1000 cm^{-1}). b. OH-stretching region (3800–3000 cm^{-1}). c. Last spectra of CO pulse (blue) and H_2 pulse (red). d. Mass spectrometry profiles of CO (m/z = 28, blue) and H_2 (m/z = 2, red) recorded during CO separation performance test at 450 °C at conditions of Fig. 1.

release and regenerated the active phase enabling the subsequent CO capture. In terms of surface species, the switch to H_2 stream resulted in a drastic reduction in intensity of the previously discussed IR bands appearing in the carbonate region, with an initial fast intensity decline during the first minute, followed by a slower decline, which is in line with the CO desorption concentration profiles observed during fixed-bed experiments (see Fig. 1). An opposite dynamic was observed in the spectral region associated with OH vibrations (Fig, 2b, 3800–3000 cm^{-1}). Broad bands in the OH region have been recognised in K/Al_2O_3 systems at temperatures up to 450 °C, indicating the persistence of surface hydroxyl groups to outgassing conditions (Kantschewa et al., 1983; Montanari et al., 2011). In this investigation, we evidenced the specific dynamic of these hydroxyl species during the capture of CO and sorbent regeneration with H_2. As shown in Fig. 2b, during the CO capture phase (0–10 min) a noticeable decline in the intensity of the OH region was observed, suggesting a transformation of the surface hydroxyl species in the sorbent. In contrast, switching to H_2 atmosphere (10–20 min) caused the sudden recovery of the OH band intensity, indicating the restoration of the OH species previously lost during CO capture.

The last DRIFTS spectra recorded during the CO and H_2 pulses are shown in Fig. 2c, providing an overview of the surface changes between the two phases. The observed dynamic of carbonate and hydroxyl surface species together suggests the presence of an active OH-containing phase, in the form of surface hydroxyl species, able to strongly interact with the polar CO molecules and sequestrate them from gas phase in the form of surface carbonates. This active phase is thus regenerated in H_2 and consumed by interaction with CO at the sorption-regeneration conditions investigated.

Considering the prominent role of the alkali component in developing the capture functionality, CO sequestration from the gas phase is thus associated with the conversion of a surface KOH-containing phase to surface carbonate species. Such transformation must involve the release of the excess H_2 in the gaseous form, following Eq. (1):

$$CO + 2KOH = K_2CO_3 + H_2 \quad (1)$$

To verify this, the composition of the reactor effluent stream was analysed by mass spectrometry during the performance test at 450 °C (See Fig. 1). Fig. 2d shows the concentration profiles corresponding of H_2 (m/z = 2) and CO (m/z = 28) during the CO capture-sorption regeneration steps. At the beginning of the capture phase (0–100 s), a clear sharp increase of the H_2 signal was observed ahead of the CO breakthrough point, indicating that the sequestration of gaseous CO in the form of surface carbonates is associated with the liberation of H_2. This result further supports the identification of a KOH-containing phase as the active intermediate in the CO sequestration to carbonates (Fig. 3I-II). The same K-derived phase was responsible for the capture of CO_2, as observed in an earlier contribution (Pinto et al., 2024), thus suggesting the compatibility of the system for simultaneous CO and CO_2 capture from complex mixtures. As previously stated, during the regeneration step, H_2 gets activated on the Cu sites, thus making the decomposition of the potassium carbonate feasible, and kinetically relevant, reversing Eq. (1) and closing the sorption cycle (Fig. 3 III-IV). Limited CO capture activity of a K/Al_2O_3 sample at 450 °C confirms the decisive role of metallic copper in the mechanism (Fig. S4). In absence of copper, the typical breakthrough profile signalling full capture of carbon monoxide was not observed. Moreover, during regeneration in H_2, the absence of the initial, high concentration peak of CO strongly points towards the ineffectiveness of H_2 alone to promote effective regeneration of the active phase for CO capture in absence of the metallic Cu component.

The operational temperature range of the CO sorption-desorption process on the Cu-K/Al_2O_3 was assessed by analysing dynamics of the surface species at different temperatures, using *in-situ* DRIFT. The results (Fig. S5) clearly indicate a temperature lower limit around 300 °C. Below this temperature, the KOH active phase is not regenerated, and

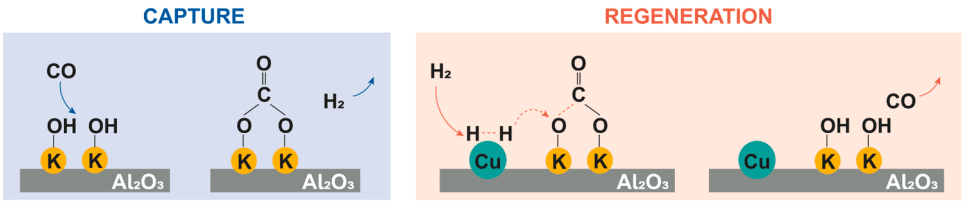

Fig. 3. Mechanism of CO capture and sorbent regeneration in H_2. Schematic representation of the different steps involved in the CO capture and sorbent regeneration in H_2. I. Capture of CO on surface hydroxyls. II. Formation of surface carbonates and liberation of gaseous H_2. III. H_2 activation on meatllic Cu and carbonates decomposition. IV. Regeneration of capture active phase and liberation of gaseous CO.

thus the cyclic operation cannot be maintained. This temperature is in line with the peak of CuO reduction in presence of K as displayed by H_2-TGA experiments (Fig. S3a) and reinforce the role of metallic Cu in providing active H species for the decomposition of the carbonate phase. This limitation in the lower operational temperature imposed by Cu is verified by a CO sorption-desorption experiment at 120 °C followed by H_2-temperature programmed reaction (TPR) of saturated sorbent (Fig. S6). Although no effective CO evolution was recorded during the regeneration steps in H_2 at 120 °C, CO was released in the H_2-TPR post-treatment upon reaching a temperature of 300 °C.

3.3. CO separation from more realistic gas streams

3.3.1. CO/N_2 separation

A critical separation challenge is the sequestration of CO from N_2-rich streams, owing to the similar molecular size and physical properties of CO and N_2. The chemical nature of the CO-sorbent interaction elucidated in the previous section provides a suitable solution for separating CO from N_2-rich streams.

Fig. 4a presents the results of the CO/N_2 separation performance test performed at 450 °C, with a CO-containing stream consisting of 0.13 vol % CO and 8.8 vol% N_2 in He. During the CO/N_2 mixture pulse (0–840 s), analysis of the reactor outlet stream by FTIR (Fig. 4a, top) and MS (m/z = 12, Fig. 4a, bottom) evidenced that the CO was fully captured by the sorbent, with no detectable CO until saturation of the sorption sites (400 s), after which a characteristic breakthrough profile for the adsorbate is observed. Conversely, N_2 is readily detected at the reactor outlet (m/z = 14, Fig. 4a, bottom) from the beginning of the pulse. The N_2 signal remains constant throughout the pulse, excluding interaction with the sorbent. During the inert He pulse (840–990 s), no release of CO was observed via FTIR/MS. The peaks observed for the fragments m/z = 14 and m/z = 12 in MS are consequence of the instantaneous pressure change in the MS chamber and do not correspond to any release from the reactor. The absence of CO release during the inert He pulse is a further confirmation of the strong chemical interaction between the CO and the active sorbent. Exposing the saturated sorbent to H_2 pulse (990–1410 s) triggered the rapid CO release, as evidenced by both FTIR and MS profiles. As expected, no N_2 release was detected, resulting in a N_2-free syngas mixture (H_2 + CO) at the outlet of the reactor during the regeneration step, demonstrating the effectiveness of this separation technology and potential application towards CO/N_2 separation purposes. In addition, suppression of the He intermediate pulse was also investigated, with the results showing that this intermediate inert stage can be omitted without affecting the process performance (Fig. S7a). The stability of the performance was tested during a 30 sorption-regeneration cycles, without any noticeable decrease in the CO capture capacity and regeneration profiles. (Fig. S7b). These results are in agreement with comparable long-term cycling stability tests performed on Cu-K/Al_2O_3 system during CO_2 capture experiments, suggesting the integrity of the material after prolonged exposure to the reaction conditions (Pinto et al., 2024).

3.3.2. CO separation in presence of H_2O and O_2

Industrially relevant CO-containing streams typically contain chemical compounds that have been reported to be significantly detrimental to CO capture technologies. Among these components, moisture (water vapor) and O_2 are commonly found in waste streams from blast furnaces and combustion processes, and their presence poses a significant challenge for conventional CO capture technologies (Bhardwaj et al., 2025). In this work, the effect of having humid CO streams and O_2 in the feed gas during the CO capture was examined.

Fig. 4b presents the temporal evolution of the CO concentration at the reactor outlet for the different steps in the adsorption-desorption cycle, for an experiment at 450 °C in which the CO-containing stream

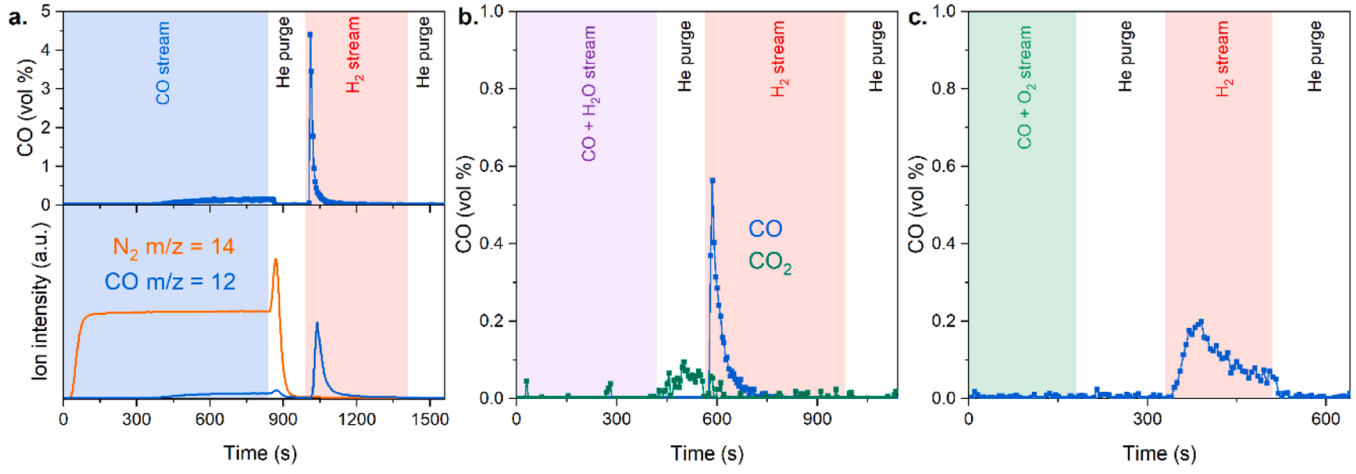

Fig. 4. CO separation from complex streams. FTIR analysis of reactor effluent during sorption-regeneration tests at 450 °C over Cu-K/Al_2O_3. a. CO/N_2 mixture (CO 0.13 vol%, N_2 8.8 vol%, rest He), He purge and pure H_2 stream. b. CO/H_2O mixture (CO 0.13 vol%, H_2O 0.3 vol%, rest He). c. CO/O_2 mixture (CO 0.13 vol%, O_2 0.5 vol%, rest He).

consists of 0.3 vol% H_2O and 0.13 vol% CO in He. The presence of water vapor did not affect the main CO capture features, with complete CO capture achieved and no further gas released during this CO capture step, similar to the dry feed case (See Fig. S8). CO desorption step in presence of H_2 took place in a similar fashion as in the dry feed case, with a fast release of CO upon exposure to the H_2 atmosphere. A closer comparison between the two cases, dry and wet CO streams, showed a lower CO concentration peak in the latter case and a seemingly slower rate of regeneration. This was attributed to the partial oxidation of Cu active sites of the sorbent material by the water vapor, which may hinder the initial H_2 activation performance of this phase. Besides, after capturing CO in presence of H_2O, a slight desorption of CO_2 during the He flush phase was noticed indicating a possible decomposition of carbonates. This desorption was likely stimulated by the persistence of H_2O in the lines during the He flush, due to the injection conditions of the experiment (See Methods). It is worth remarking that CO_2 was not present during the CO pulse, confirming the effectiveness of the capture in presence of H_2O.

Fig. 4c presents the CO concentration recorded at the reactor outlet when using a CO-containing stream composed of 0.5 vol% O_2 and 0.13 vol% CO in He at 450 °C. The results showed a complete CO uptake during CO capture step (CO pulse), despite the presence of O_2, evidencing the negligible effect of O_2 within the capture phase and the complete regeneration of the capture active sites at each cycle. Conversely, more striking differences were appreciated for the CO desorption step in presence of H_2. In this case, CO concentration showed a much broader profile, with lower peak concentration, indicating a decrease in the CO desorption rate. This phenomenon was associated with the partial oxidation of the Cu phase present in the sorbent, which limited the catalytic H_2 activation performance of the Cu phase, as observed in presence of H_2O, but with a higher impact due to the stronger oxidizing character of O_2. The hypothesis was confirmed by monitoring the evolution of H_2O vapor during the test (See Fig. S9). H_2O vapor FTIR signals presented a peak at the beginning of the regeneration phase, which fully declines before the end of the H_2 phase. Such profile can be assigned to the compete reduction of a CuO phase formed upon exposure of the metallic Cu to the O_2-containing stream.

These results are consistent with the proposed mechanism, in which K-OH species are the active sites for CO capture, and exhibit a high resistance upon exposure to humid or O_2-containing streams. The only observed effect due to handling these compounds arises from the slight oxidation of the Cu phase, responsible for H_2 activation and further potassium carbonate decomposition, which yields a slight lower CO desorption rate. Despite this lower CO desorption kinetics, the process demonstrated high robustness to the presence of water vapor and O_2 in the CO stream and showcases a promising potential as CO sequestration technology.

3.3.3. *Sorbent regeneration with H_2O*

Regeneration of the sorbent in this CO separation process is accomplished through exposure of the saturated sorbent to an H_2 stream. As discussed above, this occurs via decomposition of the formed potassium carbonate species by hydrogen activated on the Cu sites, and shared similarities with the regeneration mechanism reported for the ICCU process (Bermejo-López et al., 2019; Liu et al., 2023; Pinto et al., 2024).

In the previous section, we showed how the capture of CO in presence of limited water concentration (0.3 vol%) in the stream was feasible. At the same time, the ionic nature of the K_2CO_3 bond makes such intermediate susceptible to decomposition in presence of excess water. For this reason, the use of water vapor as a regenerating agent for the CO-saturated sorbent was investigated, and the results are presented in Fig. 5 (top graph). In this case, the sequence of gases fed to the reactor was altered by introducing a water vapor-rich pulse (10 vol% in He) within the first He purging pulse. The same experiment was repeated excluding the H_2O pulse, for comparison sake (Fig. 5, bottom graph). The exposure of the CO-saturated sorbent to the H_2O atmosphere triggered the release of CO_2, possibly following Eq. (2):

$$K_2CO_3 + H_2O = 2KOH + CO_2 \quad (2)$$

As a overall, the reaction including CO capture and selective release

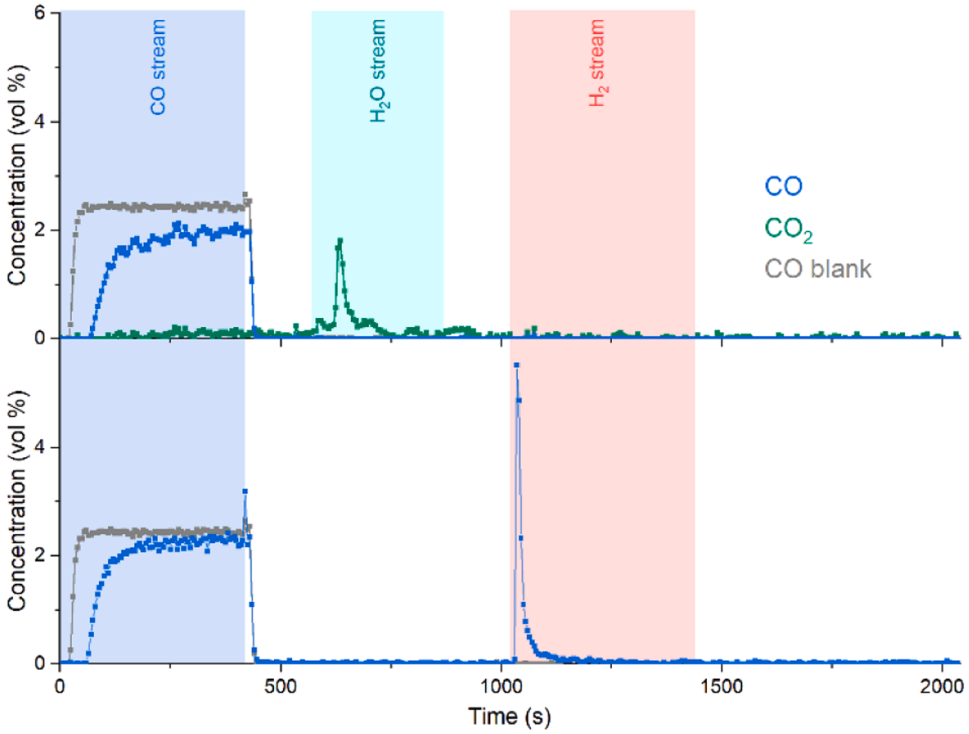

Fig. 5. Sorbent regeneration with H_2O. FTIR analysis of reactor effluent during sorption-regeneration tests at 450 °C over Cu-K/Al_2O_3 using H_2O (10 vol% in He, top graph) and pure H_2 (bottom graph).

to CO_2 upon exposure to H_2O vapor presents similarities with a sorption-mediated water-gas shift (WGS) mechanism. No CO was detected during the H_2O pulse and during the subsequent H_2 pulse, clearly evidencing a full conversion of CO to CO_2 upon exposure to H_2O. Overall, these results indicate the potentiality of regenerating the sorbent utilising water vapor-containing streams. This is confirmed also in the case of omission of the H_2 pulse (Fig. S10). In the latter case, the presence of H_2O oxidizes the Cu component but does not affect the active phase for CO capture. As a consequence, the CO capture proceeds almost unaffected but, after reaching the sorbent saturation, CO is partially converted to CO_2 by interacting with the CuO phase.

4. Conclusions

A novel CO separation technology using solid Cu-K/ Al_2O_3 dual functional materials was reported for the efficient CO sequestration and controlled release, at isothermal and isobaric conditions. A fixed bed reactor with periodic gas switching was used to experimentally study the overall CO capture and release cycle. This CO sorption-desorption process was feasible in the temperature range 300 - 450 °C with the achievement of a full CO capture scenario. Sorbent regeneration using H_2 yielded syngas (H_2 + CO), without any further chemical compound. The composition of the generated syngas could be adjusted by modifying the operation conditions, highlighting the potential of this approach for customizing H_2 to CO ratio in the generated stream.

A mechanistic investigation was conducted using *in situ* DRIFT analysis. CO capture proceeded through the formation of surface carbonates from the chemical interaction of CO with surface hydroxyls species generated by decomposition of the initial K_2CO_3 phase in H_2. Upon exposure of the saturated solid sorbent to H_2 atmosphere, H_2 activated on metallic Cu and K carbonate species were decomposed, regenerating the original K-OH active sites.

This new CO separation demonstrated a high efficiency and potential for its application towards CO/N_2 separation purposes, with the achievement of a CO-free stream during the capture phase. In addition, CO capture features were investigated in presence of water vapor and O_2, with a negligible impact on this step. Only a slight reduction of the CO desorption rate, during the regeneration stage, was observed and attributed to the partial oxidation of the Cu metal phase.

Furthermore, sorbent regeneration was feasible using high concentrations of water vapor (10 vol%), being CO_2 released from the sorbent, due to the occurrence of a WGS-like reaction. This sorption-mediated WGS reaction achieved complete CO conversion, highlighting the additional potential of this approach to achieve a higher catalytic performance as compared with conventional (co-feeding of CO and H_2) WGS reaction operation.

Declaration of competing interests

The authors are inventors on a pending patent application related to the technology described in this manuscript. The patent applicant is Delft University of Technology, with application number PCT/NL2025/150016. The authors declare that this does not influence the results or their interpretation.

CRediT authorship contribution statement

Donato Pinto: Writing – original draft, Visualization, Validation, Methodology, Investigation, Data curation, Conceptualization. **José Palomo:** Writing – review & editing, Validation, Methodology, Investigation, Data curation, Conceptualization. **Atsushi Urakawa:** Writing – review & editing, Supervision, Resources, Project administration, Methodology, Funding acquisition, Conceptualization.

Declaration of competing interest

The authors declare the following financial interests/personal relationships which may be considered as potential competing interests:

Atsushi Urakawa reports financial support provided by TU Delft. Atsushi Urakawa reports a relationship with Delft University of Technology that includes: employment. Donato Pinto, Jose Palomo, Atsushi Urakawa has patent #PCT/NL2025/150016 pending to Delft University of Technology. If there are other authors, they declare that they have no known competing financial interests or personal relationships that could have appeared to influence the work reported in this paper.

Supplementary materials

Supplementary material associated with this article can be found, in the online version, at doi:10.1016/j.ccst.2026.100670.

References

Bermejo-López, A., Pereda-Ayo, B., González-Marcos, J.A., González-Velasco, J.R., 2019. Mechanism of the CO_2 storage and *in situ* hydrogenation to CH_4. Temperature and adsorbent loading effects over Ru-CaO/Al_2O_3 and Ru-Na_2CO_3/Al_2O_3 catalysts. Appl. Catal. B Environ. 256, 117845. https://doi.org/10.1016/j.apcatb.2019.117845.

Bhardwaj, K., Kumar, D., Saji, V.S., Singh, V., Lee, Y., Lee, S., Janas, D., Mishra, Y.K., Sharma, S.K., 2025. Carbon monoxide detection, separation, and conversion into valuable products via smart nanomaterials: challenges and perspectives. Mater. Today 83, 404–445. https://doi.org/10.1016/j.mattod.2024.12.020.

Bloch, E.D., Hudson, M.R., Mason, J.A., Chavan, S., Crocellà, V., Howe, J.D., Lee, K., Dzubak, A.L., Queen, W.L., Zadrozny, J.M., Geier, S.J., Lin, L.-C., Gagliardi, L., Smit, B., Neaton, J.B., Bordiga, S., Brown, C.M., Long, J.R., 2014. Reversible CO binding enables tunable CO/H_2 and CO/N_2 separations in metal–organic frameworks with exposed divalent metal cations. J. Am. Chem. Soc. 136 (30), 10752–10761. https://doi.org/10.1021/ja505318p.

Bobadilla, L.F., Riesco-García, J.M., Penelás-Pérez, G., Urakawa, A., 2016. Enabling continuous capture and catalytic conversion of flue gas CO_2 to syngas in one process. J. CO2 Util. 14, 106–111. https://doi.org/10.1016/j.jcou.2016.04.003.

Busca, G., Lorenzelli, V., 1982. Infrared spectroscopic identification of species arising from reactive adsorption of carbon oxides on metal oxide surfaces. Mater. Chem. 7 (1), 89–126. https://doi.org/10.1016/0390-6035(82)90059-1.

Carpenter, A., 2012. CO_2 abatement in the iron and steel industry. IEA Clean Coal Centre 25, 193.

Chen, X., Song, G., Liyan, F., Li, C., Zhou, W., Hu, F., Gong, L., Kawi, S., 2026. Optimizing CuO on 3D ordered macroporous CeO_2 for CO oxidation in rich hydrogen. Rare Met 45 (2), e70115. https://doi.org/10.1002/rar2.70115.

Coenen, K., Gallucci, F., Mezari, B., Hensen, E., van Sint Annaland, M., 2018. An in-situ IR study on the adsorption of CO_2 and H_2O on hydrotalcites. J. CO2 Util. 24, 228–239. https://doi.org/10.1016/j.jcou.2018.01.008.

Delgado, M.R., Arean, C.O., 2011. Carbon monoxide, dinitrogen and carbon dioxide adsorption on zeolite H-beta: IR spectroscopic and thermodynamic studies. Energy 36 (8), 5286–5291. https://doi.org/10.1016/j.energy.2011.06.033.

Evans, A., Luebke, R., Petit, C., 2018. The use of metal–organic frameworks for CO purification. J. Mater. Chem. A 6 (23), 10570–10594. https://doi.org/10.1039/C8TA02059K.

Fedorova, E.A., Kraußer, L., Weiß, J., Fedorov, A., Brückner, A., Kondratenko, E.V., Kubis, C., 2024. Operando DRIFTS investigations on surface intermediates and effects of potassium in CO_2 hydrogenation over a K–Fe/YZrOx catalyst. ChemCatChem 16 (10), e202301697. https://doi.org/10.1002/cctc.202301697.

Filonchyk, M., Peterson, M.P., Zhang, L., Hurynovich, V., He, Y., 2024. Greenhouse gases emissions and global climate change: examining the influence of CO_2, CH_4, and N_2O. Sci. Total Environ. 935, 173359. https://doi.org/10.1016/j.scitotenv.2024.173359.

Hirai, H., Wada, K., Komiyama, M., 1983. Active Carbon-supported copper(I) chloride AS Carbon Monoxide solid adsorbent. Chem. Lett. 12 (3), 361–364. https://doi.org/10.1246/cl.1983.361.

Hyakutake, T., van Beek, W., Urakawa, A., 2016. Unravelling the nature, evolution and spatial gradients of active species and active sites in the catalyst bed of unpromoted and K/Ba-promoted Cu/Al_2O_3 during CO_2 capture-reduction. J. Mater. Chem. A 4 (18), 6878–6885. https://doi.org/10.1039/C5TA09461E.

Islamoglu, T., Chen, Z., Wasson, M.C., Buru, C.T., Kirlikovali, K.O., Afrin, U., Mian, M.R., Farha, O.K., 2020. Metal–organic frameworks against toxic chemicals. Chem. Rev. 120 (16), 8130–8160. https://doi.org/10.1021/acs.chemrev.9b00828.

James, J., Lücking, L.E., van Dijk, H.A.J., Boon, J., 2023. Review of technologies for carbon monoxide recovery from nitrogen- containing industrial streams. Front. Chem. Eng. 5. https://doi.org/10.3389/fceng.2023.1066091.

Kantschewa, M., Albano, E.V., Etrtl, G., Knözinger, H., 1983. Infrared and x-ray photoelectron spectroscopy study of K_2CO_3/γ-Al_2O_3. Appl. Catal. 8 (1), 71–84. https://doi.org/10.1016/0166-9834(83)80054-2.

Kempken, T., Hauck, T., Wang, C., De Santis, M., Szulc, W., Draxler, M., Sormann, A., Queipo, P., Miranda, M., Croon, D., Ghenda, J.T., 2021. Decarbonisation Pathways 2030 and 2050 (Deliverable D1.7). Green Steel for Europe Consortium /European Steel Technology Platform (ESTEP).

Kim, A.-R., Yoon, T.-U., Kim, S.-I., Cho, K., Han, S.-S., Bae, Y.-S., 2018. Creating high CO/CO_2 selectivity and large CO working capacity through facile loading of Cu(I) species into an iron-based mesoporous metal-organic framework. Chem. Eng. J. 348, 135–142. https://doi.org/10.1016/j.cej.2018.04.177.

Ko, K.-J., Kim, H., Cho, Y.-H., Lee, H., Kim, K.-M., Lee, C.-H., 2022. Overview of carbon monoxide adsorption performance of pristine and modified adsorbents. J. Chem. Eng. Data 67 (7), 1599–1616. https://doi.org/10.1021/acs.jced.1c00903.

Li, J., He, X., Hu, R., 2024. Integrated carbon dioxide capture and utilization for the production of CH_4, syngas and olefins over dual-function materials. ChemCatChem 16 (15), e202301714. https://doi.org/10.1002/cctc.202301714.

Li, S., Zhu, X., Wang, D., Hao, P., Zhou, F., Shi, Y., Wang, R., Cai, N., 2023. Elevated temperature adsorbents for separation applications. EnergyChem 5 (6), 100113. https://doi.org/10.1016/j.enchem.2023.100113.

Liu, G., Sun, S., Sun, H., Zhang, Y., Lv, J., Wang, Y., Zeng, J., Yan, Z., Wu, C., 2023. Integrated CO_2 capture and utilisation: a promising step contributing to carbon neutrality. Carbon Capture Sci. Technol. 7, 100116. https://doi.org/10.1016/j.ccst.2023.100116.

Ma, X., Albertsma, J., Gabriels, D., Horst, R., Polat, S., Snoeks, C., Kapteijn, F., Eral, H.B., Vermaas, D.A., Mei, B., de Beer, S., van der Veen, M.A., 2023. Carbon monoxide separation: past, present and future. Chem. Soc. Rev. 52 (11), 3741–3777. https://doi.org/10.1039/D3CS00147D.

Montanari, T., Matarrese, R., Artioli, N., Busca, G., 2011. FT-IR study of the surface redox states on platinum-potassium-alumina catalysts. Appl. Catal. B Environ. 105 (1), 15–23. https://doi.org/10.1016/j.apcatb.2011.03.021.

Nielsen, D.U., Hu, X.-M., Daasbjerg, K., Skrydstrup, T., 2018. Chemically and electrochemically catalysed conversion of CO_2 to CO with follow-up utilization to value-added chemicals. Nat. Catal. 1 (4), 244–254. https://doi.org/10.1038/s41929-018-0051-3.

Nogami, H., Yagi, J.-i., Kitamura, S.-y., Austin, P.R., 2006. Analysis on material and energy balances of ironmaking systems on blast furnace operations with metallic charging, top gas recycling and natural gas injection. ISIJ Int. 46 (12), 1759–1766. https://doi.org/10.2355/isijinternational.46.1759.

Peng, J., Xian, S., Xiao, J., Huang, Y., Xia, Q., Wang, H., Li, Z., 2015. A supported Cu(I)@MIL-100(Fe) adsorbent with high CO adsorption capacity and CO/N_2 selectivity. Chem. Eng. J. 270, 282–289. https://doi.org/10.1016/j.cej.2015.01.126.

Pinto, D., Minorello, S., Zhou, Z., Urakawa, A., 2024. Integrated CO_2 capture and reduction catalysis: role of γ-Al_2O_3 support, unique state of potassium and synergy with copper. J. Environ. Sci. 140, 113–122. https://doi.org/10.1016/j.jes.2023.06.006.

Ramírez-Santos, Á.A., Castel, C., Favre, E., 2018. A review of gas separation technologies within emission reduction programs in the iron and steel sector: current application and development perspectives. Sep. Purif. Technol. 194, 425–442. https://doi.org/10.1016/j.seppur.2017.11.063.

Saeednia, B., Sragow, A.M., Lin, Y., Sheehan, C.J., Metlay, A.S., Gau, M.R., Dye, S.A., O'Konski, S.P., Mallouk, T.E., Dmochowski, I.J., 2025. Unusually air-stable copper(I) complexes showing high selectivity for carbon monoxide. Chem. Sci. 16 (12), 5058–5063. https://doi.org/10.1039/D5SC00237K.

Scheijen, F.J.E., Ferré, D.C., Niemantsverdriet, J.W., 2009. Adsorption and dissociation of CO on body-centered cubic transition metals and alloys: effect of coverage and scaling relations. J. Phys. Chem. C 113 (25), 11041–11049. https://doi.org/10.1021/jp811130k.

Schneising, O., Buchwitz, M., Reuter, M., Weimer, M., Bovensmann, H., Burrows, J.P., Bösch, H., 2024. Towards a sector-specific CO/CO_2 emission ratio: satellite-based observations of CO release from steel production in Germany. Atmos. Chem. Phys. 24 (13), 7609–7621. https://doi.org/10.5194/acp-24-7609-2024.

Seneviratne, S.I., Donat, M.G., Pitman, A.J., Knutti, R., Wilby, R.L., 2016. Allowable CO_2 emissions based on regional and impact-related climate targets. Nature 529 (7587), 477–483. https://doi.org/10.1038/nature16542.

Smith, A.W., Quets, J.M., 1965. Adsorption of carbon monoxide on copper: infrared absorption spectra and thermodesorption. J. Catal. 4 (2), 163–171. https://doi.org/10.1016/0021-9517(65)90007-2.

Sun, H., Sun, S., Liu, T., Zeng, J., Wang, Y., Yan, Z., Wu, C., 2024. Integrated CO_2 capture and utilization: selection, matching, and interactions between adsorption and catalytic sites. ACS Catal. 14 (20), 15572–15589. https://doi.org/10.1021/acscatal.4c03861.

Veselovskaya, J.V., Derevschikov, V.S., Kardash, T.Y., Stonkus, O.A., Trubitsina, T.A., Okunev, A.G., 2013. Direct CO_2 capture from ambient air using K_2CO_3/Al_2O_3 composite sorbent. Int. J. Greenh. Gas Control 17, 332–340. https://doi.org/10.1016/j.ijggc.2013.05.006.